IOPscience iopscience.iop.org

Home Search Collections Journals About Contact us My IOPscience

Elastodynamic cloaking and field enhancement for soft spheres

This content has been downloaded from IOPscience. Please scroll down to see the full text.

2016 J. Phys. D: Appl. Phys. 49 445101

(http://iopscience.iop.org/0022-3727/49/44/445101)

View the table of contents for this issue, or go to the journal homepage for more

Download details:

IP Address: 194.167.230.226
This content was downloaded on 19/01/2017 at 17:31

Please note that terms and conditions apply.

You may also be interested in:

Metamaterials beyond electromagnetism
Muamer Kadic, Tiemo Bückmann, Robert Schittny et al.

Non-singular cloaks allow mimesis
André Diatta and Sébastien Guenneau

Partial elastodynamic cloaking by means of fiber-reinforced composites
P Olsson and David J N Wall

A homogenization route towards square cylindrical acoustic cloaks
Mohamed Farhat, Sébastien Guenneau, Stefan Enoch et al.

On three-dimensional spherical acoustic cloaking
Ligia Munteanu and Veturia Chiroiu

Transformation quantum optics: designing spontaneous emission using coordinate transformations
Jingjing Zhang, Martijn Wubs, Pavel Ginzburg et al.

Acoustic cloaking transformations from attainable material properties
Yaroslav Urzhumov, Fabrizia Ghezzo, John Hunt et al.

Cyclic concentrator, carpet cloaks and fisheye lens via transformation plasmonics
M Alaoui, K Rustomji, T M Chang et al.

OPEN ACCESS
IOP Publishing
Journal of Physics D: Applied Physics
J. Phys. D: Appl. Phys. **49** (2016) 445101 (15pp)
doi:10.1088/0022-3727/49/44/445101

Elastodynamic cloaking and field enhancement for soft spheres

Andre Diatta and Sebastien Guenneau

Aix-Marseille Univ., CNRS Centrale Marseille, Institut Fresnel, 13013 Marseille, France

E-mail: andre.diatta@fresnel.fr, andrediatta@gmail.com

Received 22 May 2015, revised 9 August 2016
Accepted for publication 11 August 2016
Published 7 October 2016

Abstract

We propose a spherical cloak described by a non-singular asymmetric elasticity tensor $\mathbb{C}$ depending upon a small parameter η, that defines the softness of a region one would like to conceal from elastodynamic waves. By varying η, we generate a class of soft spheres dressed by elastodynamic cloaks, which are shown to considerably reduce the scattering of the soft spheres. Importantly, such cloaks also provide some wave protection except for a countable set of frequencies, for which some large elastic field enhancement can be observed within the soft spheres. Through an investigation of trapped modes in elasticity, we supply a good approximation of such Mie-type resonances by some transcendental equation. Our results, unlike previous studies that focused merely on the invisibility aspects, shed light on potential pitfalls of elastodynamic cloaks for earthquake protection designed via geometric transforms: a seismic cloak needs to be designed in such a way that its inner resonances differ from eigenfrequencies of the building one wishes to protect. In order to circumvent this downfall of field enhancement inside the cloaked area, we introduce a novel generation of cloaks, named here, mixed cloaks. Such mixed cloaks consist of a shell that detours incoming waves, hence creating an invisibility region, and of a perfectly matched layer (PML, located at the inner boundary of the cloaks) that absorbs residual wave energy in such a way that aforementioned resonances in the soft sphere are strongly attenuated.

The designs of mixed cloaks with a non-singular elasticity tensor combined with an inner PML and non-vanishing density bring seismic cloaks one step closer to a practical implementation. Note in passing that the concept of mixed cloaks also applies in the case of singular cloaks and can be translated in other wave areas for a similar purpose (i.e. to smear down inner resonances within the invisibility region).

Keywords: seismic metamaterials, seismic protection by cloaking, invisibility cloak in civil engineering, Cosserat elastic material, mixed cloak for elastic waves, trapped modes in elastodynamic cloaking, perfectly matched layers in transformation elastodynamics

(Some figures may appear in colour only in the online journal)

1. Introduction

Ten years ago, two groups of physicists unveiled theoretical paths towards the design of invisibility cloaks for electromagnetic waves, by making geometric transforms in Maxwell's [1] and Helmholtz's [2] equations. Such transforms conceal a region of space (e.g. by blowing up a point to a circle, or a sphere). This prompted mathematicians to investigate coordinate changes in other wave equations, notably the Navier equations for elastic waves [3]. The main difference between Maxwell's and Navier's equations is that the former retain their form under coordinate changes, unlike the latter. Notably, in [4] the design of a cylindrical cloak for in-plane elastic waves with an asymmetric elasticity tensor resulting

Original content from this work may be used under the terms of the Creative Commons Attribution 3.0 licence. Any further distribution of this work must maintain attribution to the author(s) and the title of the work, journal citation and DOI.

from a radially symmetric geometric transform was investigated numerically as a modified version of the Willis' type [5] transformed equations derived in [3]. The seemingly irreconcilable structures of transformed Navier equations studied in [3, 4] were later encompassed within a more general elasticity framework [6]. In parallel to the developments of these theoretical and numerical works, engineering science has gained a prominent position in the metamaterials' community, as more and more groups worldwide get to work on the design, fabrication and characterization of so-called acoustic metamaterials [7]. Notably, the water wave [8] and acoustic [9–13] cloaks have been investigated. Acoustic metamaterials for lensing [14] and other transformation based imaging systems have given rise to a flourishing literature [7]. Regarding bulk elastic waves, some theoretical [15–17] and experimental [18] progress has been made in the control of flexural elastic waves in thin plates. In that case, the transformed governing equations (e.g. Kirchhoff) have a simpler structure which helps engineer structured cloaks.

In the present article, we investigate spherical cloaks for solid elastic waves using a radially symmetric linear one-to-one geometric transform that depends upon a positive parameter η no greater than 1. See figures 1(A) and (B) for schematic illustrations. The resulting cloak models an elastodynamic medium, with nonsingular elasticity tensor and finite nowhere zero scalar mass density, that can be viewed as a generalization of the work [19]. The latter corresponds to the case when the parameter η is zero. However, in [19] we assumed some stress-free boundary conditions on the inner boundary of the cloak so that one cannot observe the phenomenon of wave protection within that paper. We note that, for small values of the parameter η, the cloaked region is a soft sphere, which is hence sensitive to any field that may possibly bypass the cloak and penetrate it. Let us stress that an object placed within the cloak is completely invisible to an external observer, hence it is different from shrinking devices studied by some authors [20].

We discuss their underlying mechanism and illustrate the theory using a finite element approach which is adequate to solve the Navier equations in transformed anisotropic heterogeneous media with asymmetric elasticity tensors.

The numerical exploration unveils a countable set of resonant eigenfrequencies, for which the elastic field is enhanced (trapped elastic modes) within the soft spheres, thereby making protection, say, against seismic waves, not a trivial consequence of cloaking.

However, the cloaks provide some wave protection outside such a countable set of Mie-type resonances that are well approximated by some transcendental equation (15). We propose a new generation of cloaks, the mixed cloaks, as a way to circumvent this downfall of field enhancement inside the cloaked area at specific resonances. Figure 1(C) gives a schematic picture of the geometric construction of mixed cloaks. These consist of two concentric spherical shells sharing a boundary. The first (outer) shell acts as an ordinary elastodynamic cloak, that is, it detours incoming waves so that, the enclosed region becomes an invisibility region. The second (inner) shell is a perfectly matched layer that absorbs residual wave energy in such a way that aforementioned resonances in the (enclosed) soft sphere are strongly attenuated. Let us emphasize that here we use PML not as a computational tool to model unbounded domains as in section 4.1, but rather as a mean to attenuate (without reflection) a wave within the cloak. In practice, one could achieve mixed cloaks through a homogenization algorithm for both the PML and the cloak. The fact that these two shells are described by asymmetric elasticity tensors means that classical homogenization would fail, but there exists some subtle way to approach the ideal PML and cloak parameters by layers of symmetric, homogeneous and isotropic elastic media [21].

The propagation of elastic waves is governed by the Navier equations. Assuming time harmonic $\exp(-\mathrm{i}\omega t)$ dependence, with ω as the angular wave frequency and t the time variable, allows us to work directly in the spectral domain. Such dependence is assumed henceforth and suppressed leading, in spherical coordinates, to

$$\begin{aligned}
-\sqrt{-1}\ \omega\, p_r &= \frac{1}{r^2}\frac{\partial}{\partial r}(r^2\sigma_{rr}) + \frac{1}{r}\left(\frac{\cos\theta}{\sin\theta} + \frac{\partial}{\partial\theta}\right)\sigma_{\theta r} \\
&\quad - \frac{1}{r}\sigma_{\theta\theta} + \frac{1}{r\sin\theta}\frac{\partial}{\partial\phi}\sigma_{\phi r} - \frac{1}{r}\sigma_{\phi\phi} \\
-\sqrt{-1}\ \omega\, p_\theta &= \frac{1}{r^2}\frac{\partial}{\partial r}(r^2\sigma_{r\theta}) + \frac{1}{r}\left(\frac{\cos\theta}{\sin\theta} + \frac{\partial}{\partial\theta}\right)\sigma_{\theta\theta} \\
&\quad + \frac{1}{r}\sigma_{\theta r} + \frac{1}{r\sin\theta}\frac{\partial}{\partial\phi}\sigma_{\phi\theta} - \frac{\cos\theta}{r\sin\theta}\sigma_{\phi\phi} \\
-\sqrt{-1}\ \omega\, p_\phi &= \frac{1}{r^2}\frac{\partial}{\partial r}(r^2\sigma_{r\phi}) + \frac{1}{r}\left(\frac{\cos\theta}{\sin\theta} + \frac{\partial}{\partial\theta}\right)\sigma_{\theta\phi} \\
&\quad + \frac{1}{r}\sigma_{\phi r} + \frac{\cos\theta}{r\sin\theta}\frac{\partial}{\partial\phi}\sigma_{\phi\theta} + \frac{1}{r\sin\theta}\sigma_{\phi\phi}
\end{aligned} \tag{1}$$

where the quantity of motion $\mathbf{p} = (p_j)$ and the stress tensor $\boldsymbol{\sigma} = (\sigma_{ij})$ are related to the displacement field $\mathbf{u} = (u_j)$ via

$$\sigma_{ij} = C_{ijkl}\,(\nabla\mathbf{u})_{kl},\ p_j = -\sqrt{-1}\ \omega\ \rho\ u_j, \tag{2}$$

with $i, j, k, l = r, \theta, \phi$, where $\mathbb{C} := (C_{ijkl})$ is the rank-four elasticity tensor, $\nabla\mathbf{u}$ is the deformation tensor, see (A.1), and ρ the scalar density of the elastic medium.

From now on, we consider equation (1) in an isotropic homogeneous elastic medium with Lamé parameters λ and μ, so that $\mathbb{C}$ has the following 21 non-zero coefficients: $C_{iiii} = \lambda + 2\mu$ and if $i \neq j$, $C_{iijj} = \lambda$, $C_{ijij} = C_{ijji} = \mu$. See appendix A.

Following [6], let us consider the coordinate change $\mathbf{x} = (r, \theta, \phi) \longmapsto \mathbf{x}' = (r', \theta', \phi')$ and assume that the resulting transformed displacement $\mathbf{u}' = \mathbf{u}'(r', \theta', \phi')$ is linearly related to $\mathbf{u}$ as $\mathbf{u} = \mathbf{A}^T\mathbf{u}'$, with $\mathbf{A}$ a matrix field in general. Below, we will let $\mathbf{S}$ and $\mathbf{D}$ denote some third order tensors possibly encompassing an ω dependence. The above coordinate change leads to a transformed equation

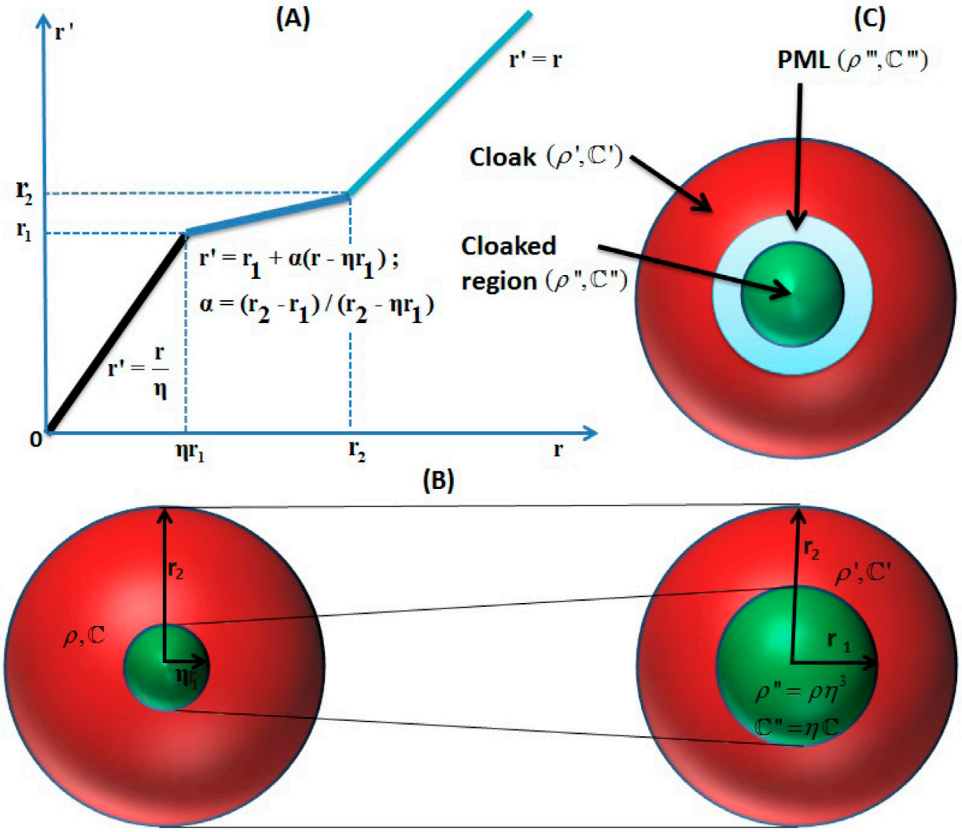

Figure 1. Illustration of geometric transform (6) with (A) its graph as a broken line and (B) the subsequent stretch of elastic space from $\mathbf{x} = (r, \theta, \phi)$ (left) to $\mathbf{x}' = (r', \theta', \phi')$ (right), where r_1 and r_2 are the inner and outer radii of the spherical cloak, respectively. In terms of material parameters a small sphere of radius ηr_1 coated with a hollow sphere of outer radius r_2 (left) both of which with an isotropic homogeneous symmetric elastic constitutive tensor $\mathbb{C}$ and a homogeneous scalar density ρ, are mapped onto a larger sphere of radius r_1 with an isotropic homogeneous symmetric elastic constitutive tensor $\mathbb{C}'' = \eta\mathbb{C}$ and a homogeneous scalar density $\rho'' = \rho\eta^3$, which is coated by a hollow sphere of radius r_2 with a heterogeneous asymmetric elastic constitutive tensor $\mathbb{C}'$, see (8) and a heterogeneous scalar density ρ', see (7). In (C), a schematic picture of the construction of a mixed cloak is shown: it is based on the cloak in (B) however with an inner boundary which has a PML attached to it in order to smear down residual elastodynamic energy within the invisibility region. Note that the inner sphere (cloaked region) consists of an isotropic homogeneous elastic medium with a symmetric elastic constitutive tensor $\mathbb{C}''$, whereas both PML and cloak have asymmetric heterogeneous elasticity tensors $\mathbb{C}'''$ and $\mathbb{C}'$ and heterogeneous scalar densities ρ''' and ρ'.

$$
\begin{aligned}
-\sqrt{-1}\ \omega\, p'_{r'} &= \frac{1}{r'^2}\frac{\partial}{\partial r'}(r'^2\sigma'_{r'r'}) + \frac{1}{r'}\left(\frac{\cos\theta'}{\sin\theta'} + \frac{\partial}{\partial\theta'}\right)\sigma'_{\theta'r'} \\
&\quad - \frac{1}{r'}\sigma'_{\theta'\theta'} + \frac{1}{r'\sin\theta'}\frac{\partial}{\partial\phi'}\sigma'_{\phi'r'} - \frac{1}{r'}\sigma'_{\phi'\phi'} \\
-\sqrt{-1}\ \omega\, p'_{\theta'} &= \frac{1}{r'^2}\frac{\partial}{\partial r'}(r'^2\sigma'_{r'\theta'}) + \frac{1}{r'}\left(\frac{\cos\theta'}{\sin\theta'} + \frac{\partial}{\partial\theta'}\right)\sigma'_{\theta'\theta'} \\
&\quad + \frac{1}{r'}\sigma'_{\theta'r'} + \frac{1}{r'\sin\theta'}\frac{\partial}{\partial\phi'}\sigma'_{\phi'\theta'} - \frac{\cos\theta'}{r'\sin\theta'}\sigma'_{\phi'\phi'} \\
-\sqrt{-1}\ \omega\, p'_{\phi'} &= \frac{1}{r'^2}\frac{\partial}{\partial r'}(r'^2\sigma'_{r'\phi'}) + \frac{1}{r'}\left(\frac{\cos\theta'}{\sin\theta'} + \frac{\partial}{\partial\theta'}\right)\sigma'_{\theta'\phi'} \\
&\quad + \frac{1}{r'}\sigma'_{\phi'r'} + \frac{\cos\theta'}{r'\sin\theta'}\frac{\partial}{\partial\phi'}\sigma'_{\phi'\theta'} + \frac{1}{r'\sin\theta'}\sigma'_{\phi'\phi'},
\end{aligned}
\tag{3}
$$

whereby the transformed $\mathbf{p}' = (p'_{j'})$, stress tensor $\boldsymbol{\sigma}' = (\sigma'_{i'j'})$, rank-four elasticity tensor $\mathbb{C}' = (C'_{i'j'k'l'})$ and density $\rho' = (\rho'_{i'j'})$, are now related to the transformed displacement $\mathbf{u}' = \mathbf{u}'(r', \theta', \phi')$, by

$$
\begin{aligned}
\sigma'_{i'j'} &= C'_{i'j'k'l'}\,(\nabla'\mathbf{u}')_{k'l'} + S_{i'j'l'}u'_{l'}, \\
p'_{j'} &= D_{j'k'l'}(\nabla'\mathbf{u}')_{k'l'} - \sqrt{-1}\ \omega\ \rho'_{j'l'}u'_{l'},
\end{aligned}
\tag{4}
$$

with $i', j', k', l' = r', \theta', \phi'$ and ∇' the transformed gradient written in transformed coordinates. One notes that the transformed stress $\boldsymbol{\sigma}'$ is generally not symmetric and the density ρ' is now a second order tensor. In order to preserve the symmetry of the stress tensor, one has to assume [6] that $\mathbf{A}$ is a multiple of the Jacobian matrix $\partial\mathbf{x}'/\partial\mathbf{x}$ of the transformation, i.e $A_{ij} = \xi(\partial\mathbf{x}'/\partial\mathbf{x})_{ij}$, where ξ is a non-zero scalar, in which case one obtains a Willis-type equation [3, 5]. However, another special case of $\mathbf{A}$ for which the elasticity tensor $\mathbb{C}'$ does not have the minor symmetries (Cosserat Material [35]), but the stretched density ρ' is now a scalar field (unlike in the work by [3]), is when $\mathbf{A}$ is the identity matrix $\mathbf{I}$, which leads to [4, 19] $\mathbf{u}' = \mathbf{u}$ and

$$
\begin{aligned}
\sigma'_{i'j'} &= C'_{i'j'k'l'}\,(\nabla'\mathbf{u}')_{k'l'}, \\
p'_{j'} &= -\sqrt{-1}\ \omega\ \rho' u'_{j'},
\end{aligned}
\tag{5}
$$

where the body force is assumed to be zero.

This equation is derived from (4) by noting that $\mathbf{S} = \mathbf{D} = \mathbf{0}$ when $\mathbf{A} = \mathbf{I}$, see [6]. In the sequel, we work in the framework of (3) coupled with (5).

2. Kohn's transform for non singular elastic cloaks

Let us now consider the geometric transform,

$$r' = \begin{cases} \dfrac{r}{\eta}, \text{if } 0 \leqslant r \leqslant \eta r_1 \\ r_1 + \dfrac{r_2 - r_1}{r_2 - \eta r_1}(r - \eta r_1), \text{if } \eta r_1 \leqslant r \leqslant r_2 \\ r, \text{if } r \geqslant r_2 \end{cases} \tag{6}$$

which was first introduced in the context of cloaking in the conductivity equation [22], where $\theta' = \theta$, $\phi' = \phi$. This geometric transform maps, in a one-to-one smooth way, a sphere $0 \leqslant r \leqslant \eta r_1$ of radius ηr_1 onto the sphere $0 \leqslant r \leqslant r_1$ and the shell $\eta r_1 \leqslant r' \leqslant r_2$, onto the shell $r_1 \leqslant r' \leqslant r_2$, as illustrated in figures 1(A) and (B). In the cylindrical case, design of transformation-based Cosserat elastic cloaks has been first discussed in [4] , where it only involved a tensor $\mathbb{C}'$ with 8 non-vanishing coefficients. In the present spherical case, we need to consider a tensor $\mathbb{C}'$ with 21 non-vanishing coefficients [19]. Moreover, the displacement field has three components in our case. By application of transformation (6) in the region $0 \leqslant r \leqslant r_2$, the Navier equation (1) together with relations (2) are mapped onto the equation (3) coupled with (5), with

$$\rho' = ab^2(r')\,\rho, \tag{7}$$

where $a = \frac{r_2 - \eta r_1}{r_2 - r_1}$ and $b(r') = \frac{(r' - r_1)}{r'}a + \frac{\eta r_1}{r'}$, and the elasticity tensor $\mathbb{C}'$ has 21 non-zero spherical components (it is illuminating to compare these coefficients with those of a fully symmetric elasticity tensor for an isotropic homogeneous medium that we recall in appendix A, see equation (A.1)), namely

$$\begin{aligned}
&C'_{r'r'r'r'} = (\lambda + 2\mu)\frac{b^2(r')}{a}, C'_{\theta\theta\theta\theta} = C'_{\phi\phi\phi\phi} = (\lambda + 2\mu)a, \\
&C'_{r'r'\theta\theta} = C'_{\theta\theta r'r'} = C'_{r'r'\phi\phi} = C'_{\phi\phi r'r'} = \lambda b(r'), \\
&C'_{\theta\theta\phi\phi} = C'_{\phi\phi\theta\theta} = \lambda a,\ C'_{r'\theta r'\theta} = C'_{r'\phi r'\phi} = \frac{b^2(r')}{a}\mu, \\
&C'_{\theta r'\theta r'} = C'_{\theta\phi\theta\phi} = C'_{\phi r'\phi r'} = C'_{\phi\theta\phi\theta} = a\mu, \\
&C'_{r'\theta\theta r'} = C_{\theta r'r'\theta} = C'_{r'\phi\phi r'} = C'_{\phi r'r'\phi} = b(r')\mu, \\
&C'_{\theta\phi\phi\theta} = C'_{\phi\theta\theta\phi} = a\mu.
\end{aligned} \tag{8}$$

Inside the resulting ball of radius r_1, the density and elasticity tensor, here denoted by ρ'' and $\mathbb{C}''$ respectively, are obtained from formulas (7) and (8) by setting $a = \eta = b$. Namely,

$$\rho'' = \eta^3\,\rho, \tag{9}$$

and $\mathbb{C}'' = \eta\mathbb{C}$, that is $\mathbb{C}''$ is isotropic, homogeneous and fully symmetric, with 21 non-zero spherical components:

$$\begin{aligned}
&C''_{r'r'r'r'} = C''_{\theta\theta\theta\theta} = C''_{\phi\phi\phi\phi} = (\lambda + 2\mu)\eta, \\
&C''_{r'r'\theta\theta} = C''_{\theta\theta r'r'} = C''_{r'r'\phi\phi} = C''_{\phi\phi r'r'} = C''_{\theta\theta\phi\phi} \\
&= C''_{\phi\phi\theta\theta} = \lambda\eta, \\
&C''_{r'\theta r'\theta} = C''_{r'\phi r'\phi} = C''_{\theta r'\theta r'} = C''_{\theta\phi\theta\phi} \\
&= C''_{\phi r'\phi r'} = C''_{\phi\theta\phi\theta} = C''_{r'\theta\theta r'} = C''_{\theta r'r'\theta} \\
&= C''_{r'\phi\phi r'} = C''_{\phi r'r'\phi} = C''_{\theta\phi\phi\theta} = C''_{\phi\theta\theta\phi} = \mu\eta.
\end{aligned} \tag{10}$$

3. Physical discussion of the structure of the elasticity tensor

One notes that when $\eta = 0$, (7) and (8) have the same form as in [19] as Kohn's transform [22] coincides with Pendry's transform [1] and when $\eta = 1$, Kohn's transform reduces to the identity so that (7)–(10) all have the same entries as the elasticity tensor of the surrounding medium. As discussed above, one should note that the minor symmetries are broken and $b(r_1) = \eta$ which means $C'_{\theta\theta\theta\theta}/C'_{r'r'r'r'} = C'_{\phi\phi\phi\phi}/C'_{r'r'r'r'}$ is $\frac{1}{\eta^2}$ at the inner boundary of the cloak (anisotropy of $\frac{1}{\eta^2}$), unlike in our previous work [19], wherein the anisotropy was infinite (since η was equal to zero). Moreover, the off-diagonal components are also constant at the boundary $r' = r_1$, they are nonzero whenever $\eta \neq 0$. The physical interpretation is that shear and pressure waves propagate much faster (the smaller η, the faster) in the azimuthal and elevation directions than in the radial direction on the surface of the inner boundary. In fact, the waves' acceleration in azimuthal and elevation directions makes possible a vanishing phase shift between an elastic wave propagating in an isotropic homogeneous elastic medium, and another one propagating around the core region (without this acceleration, it is clear that the longer wave trajectory in the latter case would induce a deformed wavefront in forward scattering, see e.g. the shadow region in the lower panels of figure 6). One should also note that there are no infinite entries within the elasticity tensor, unlike for the cylindrical cloak studied in [4]. Let us further note that comparing (8) and (10) at $r' = r_1$, for $i, j = r', \theta, \phi$ and $i \neq j$, we have $C'_{ijij} = C''_{ijij} = \lambda\eta$ and $C'_{ijji} = C'_{ijij} = C''_{ijji} = C''_{ijij} = \mu\eta$, which means that these entries of the transformed elasticity tensor are continuous across the interface $r' = r_1$. However, $C'_{rrrr}/C''_{rrrr} = \eta/a$ and $C'_{\theta\theta\theta\theta}/C''_{\theta\theta\theta\theta} = C'_{\phi\phi\phi\phi}/C''_{\phi\phi\phi\phi} = a/\eta$ ($\mathbb{C}''$ is the tensor in the inner ball). This is in accordance with the fact that the elasticity tensor $\mathbb{C}'$ is strongly anisotropic in the azimuthal and elevation directions, whereas $\mathbb{C}''$ is isotropic and has entries of order η.

Let us now note that when $r = r_2$, the geometric transform (6) leads to $r' = r_2$. In this case, the transformed density is $\rho' = a\rho$ as $b(r_2) = 1$ and the diagonal components of the transformed elasticity tensor reduce to $C'_{r'r'r'r'} = (\lambda + 2\mu)/a, C'_{\theta\theta\theta\theta} = C'_{\phi\phi\phi\phi} = (\lambda + 2\mu)a$, hence $C'_{r'r'r'r'} = C_{rrrr}/a$, $C'_{\theta\theta\theta\theta} = aC_{\theta\theta\theta\theta}$ and $C'_{\phi\phi\phi\phi} = aC_{\phi\phi\phi\phi}$ on the outer boundary of the cloak. This expresses the fact that a stretch along the radial direction is compensated by a contraction along the azimuthal and elevation directions in such a way that elastic media (cloak and surrounding isotropic elastic medium) are impedance-matched at $r' = r_2$. The cloak's outer boundary therefore behaves in many ways as an impedance matched 'thin' elastic layer. However, we note that the components of $\mathbb{C}'$ pose no limitations on the applied frequency ω from low to high frequency, unlike for the case of coated cylinders studied back in 1998 in the context of elastic neutrality by Bigoni *et al* [23]. The fact that $\mathbb{C}'$ does not depend on ω, i.e. the cloak consists of a non-dispersive elastic medium, makes it work at all frequencies, but one should keep in mind that any structured medium designed to approximate the ideal cloak's parameters (e.g. via

homogenization) would necessarily involve some dispersion, and thus limit the interval of frequencies over which the cloak can work. Such a feature has been already observed in [16, 18], for cloaking of flexural waves in thin-elastic plates.

4. Numerical implementation and illustrations

Let us now numerically investigate the cloaking efficiency. In order to do this, we implement the 3^4 spatially varying entries of the transformed tensor in Cartesian coordinates in the finite element package COMSOL MULTIPHYSICS. We mesh the computational domain using 1105 932 tetrahedral elements, 36 492 triangular elements, 1128 edge elements and 25 vertex elements. This domain consists of an isotropic homogeneous elastic medium within a sphere of radius $r_3 = 10$ m, containing a small sphere (an isotropic homogeneous medium) of radius $r_1 = 2$ m surrounded by the cloak (a heterogeneous, anisotropic elastic metamaterial in a spherical shell of inner radius $r_1 = 2$ m and outer radius $r_2 = 4$ m) and a point force oriented along the direction (1,1,1), which is located at (4 m, −7 m, 0 m), where (0,0,0) is the center of the cloak. The sphere of radius $r_3 = 10$ m is itself surrounded by a spherical shell of inner radius r_3 and outer radius $r_4 = 12$ m, which is filled with an anisotropic homogeneous absorptive medium of the Cosserat type acting as a (reflectionless) perfectly matched layer (PML).

4.1. Elastic spherical perfectly matched layers

In this section, we supply a fully detailed (i.e. complete) expression for the spherical elastic perfectly matched layers of cosserat type. We consider the radial function $s_r(r) = 1 - i$ and deduce elastic spherical PML from the geometric transform

$$r'' = r_3 + \int_{r_3}^{r} s_r(v)\mathrm{d}v, \ \theta'' = \theta, \ \phi'' = \phi. \tag{11}$$

This transform leads, in the same way as (6) did for $\mathbb{C}'$ and ρ', to a homogeneous anisotropic asymmetric elasticity tensor $\mathbb{C}'''$ and a scalar (homogeneous) density ρ''', with

$$\begin{aligned}
&C'''_{r'r'r'r'} = \frac{(1+i)}{2}(\lambda + 2\mu), C'''_{\theta\theta\theta\theta} = C'''_{\phi\phi\phi\phi} = (1-i)(\lambda+2\mu),\\
&C'''_{r'r'\theta\theta} = C'''_{\theta\theta r'r'} = C'''_{r'r'\phi\phi} = C'''_{\phi\phi r'r'} = \lambda,\\
&C'''_{\theta\theta\phi\phi} = C'''_{\phi\phi\theta\theta} = (1-i)\lambda, \ C'''_{r'\theta r'\theta} = C'''_{r'\phi r'\phi} = \frac{(1+i)}{2}\mu,\\
&C'''_{\theta r'\theta r'} = C'''_{\theta\phi\theta\phi} = C'''_{\phi r'\phi r'} = C'''_{\phi\theta\phi\theta} = (1-i)\mu,\\
&C'''_{r'\theta\theta r'} = C'''_{\theta r'r'\theta} = C'''_{r'\phi\phi r'} = C'''_{\phi r'r'\phi} = \mu,\\
&C'''_{\theta\phi\phi\theta} = C'''_{\phi\theta\theta\phi} = (1-i)\mu.
\end{aligned} \tag{12}$$

where, again, λ and μ are the Lamé coefficients of the ambient homogeneous and isotropic space, and $\rho''' = (1-i)\rho$. Since the elastic waves are damped inside the PML and reach the outer boundary of the shell with a vanishing amplitude, we set either clamped or traction free boundary conditions at $r'' = r_4$ (we have checked this does not affect the numerical result).

4.2. Finite element results

One should keep in mind that any numerical implementation in a finite element package requires a Cartesian coordinate system. In our case, we used COMSOL where the transformed elastic tensors $\mathbb{C}'$ for the cloak and $\mathbb{C}'''$ for the PML had up to 81 non-vanishing spatially varying entries. A good way to detect any flaw in the numerical implementation is to compare the solution to the problem for a time harmonic point source in an isotropic homogeneous medium (supplied with spherical elastic PML), see the center panel for $\eta = 1$ in figure 6, with the solution to the same problem when we have cloaks surrounding certain soft spheres, as shown in other panels in figure 6, where we vary the η parameter in the range 0.001 (extremely soft sphere and cloak with nearly singular strongly anisotropic elasticity tensor with marked minor symmetry breaking) to 0.5 (mildly soft sphere with weakly anisotropic and asymmetric elasticity tensor). The magnitude of the elastic displacement outside the cloaks is virtually indistinguishable from that of the center panel (case $\eta = 1$).

For $\omega = 3$ rad $\cdot$ s^{-1} and $\eta = 0.1$, one can see in figures 2 and 3 that the deformation of the elastic medium outside the cloak is nearly identical to that of the isotropic homogeneous elastic medium (we use the normalized density $\rho = 1$ and Lamé parameters $\mu = 1$ and $\lambda = 2.3$, for respectively the shear modulus and the compressibility). By comparison, the deformation of the elastic medium is clearly visible for the soft sphere (of normalized density $\rho = \eta^3$ and Lamé parameters $\mu = \eta$ and $\lambda = 2.3\eta$) without the cloak.

The small discrepancy between the upper and lower panels in figure 2, third column, is attributed to the artificial anisotropy induced by the mesh (it is not radially symmetric, see [19]) and the small absorption due to PMLs.

Plots of elastic deformation can be somewhat misleading, and we therefore add plots of the magnitude of the elastic displacement field, for $\eta = 0.1$, in figure 4 (scattering by a soft sphere) and figure 5 (scattering by a soft sphere surrounded by the cloak) both for angular frequencies varying in the range 2–4.5 rad $\cdot$ s^{-1}, where it should be noticed that the shaded region behind the soft sphere in figure 4 (drop of wave amplitude and phase shift), is almost completely removed in figure 5 thanks to the cloak. Upon inspection of these two figures, one can clearly see that the elastic field scattered by a soft sphere clothed with the cloak is virtually indistinguishable from bare isotropic elastic space.

However, these results may not be representative of the cloak's behavior at other frequencies. It is also possible that other parameters η lead to cloaks offering a better wave protection. Figure 6 shows the magnitude of the displacement field for $\omega = 3$ rad $\cdot$ s^{-1} and for 7 values of η ranging from 0.001 to 0.5.

It seems plausible that the elastic wave displacement vanishes inside the cloaked region, but this is in contradistinction with plots of elastic field magnitude in figures 5 and 6. It is also important to have some quantitative criterion regarding the possible wave protection inside the cloaked region (the soft sphere within the cloak). In order to check more thoroughly what is the level of wave protection depending upon the wave frequency and the value of η (in a two-parameter

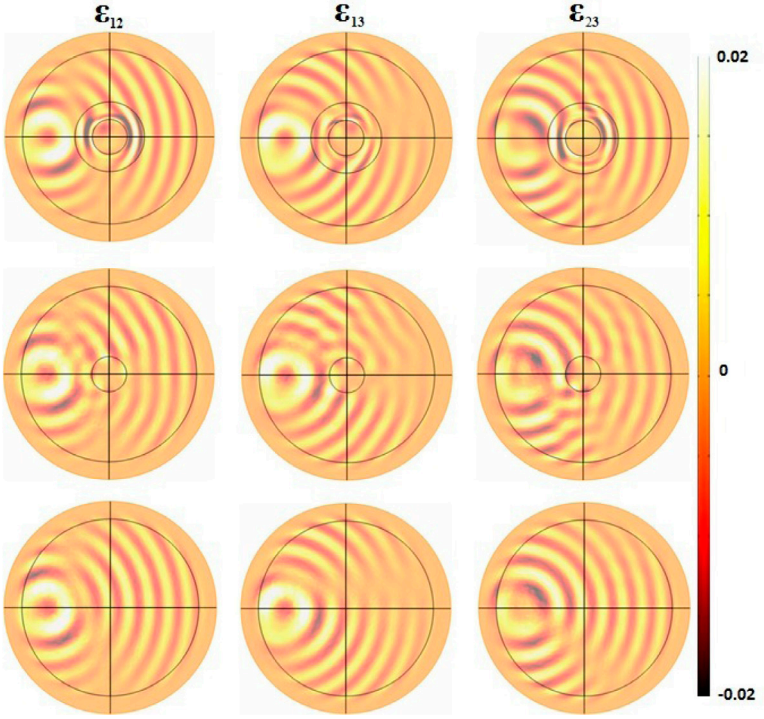

Figure 2. Deformation of a homogeneous isotropic elastic medium $\mu = 1$, $\lambda = 2.3$ and $\rho = 1$ (lower panel); Deformation of the same medium now containing a soft homogeneous isotropic spherical obstacle of radius 2 m with Lamé parameters $\mu = \eta$, $\lambda = 2.3\eta$ and $\rho = \eta^3$ for $\eta = 0.1$ (middle panel); Deformation of the same obstacle but now surrounded by a heterogeneous elastic cloak with an elasticity tensor without the minor symmetries (upper panel) of inner radius $r_1 = 2$ m and outer radius $r_2 = 4$ m, subjected to a concentrated load of polarization (1,1,1) with frequency $\omega = 3\,\mathrm{rad}\cdot\mathrm{s}^{-1}$ located in a homogeneous isotropic medium (see upper panel) at a distance 8.062 m from the origin. Real part of the deformation components $\epsilon_{12} = \frac{1}{2}(\frac{\partial u_1}{\partial x_2} + \frac{\partial u_2}{\partial x_1})$ (left column), $\epsilon_{13} = \frac{1}{2}(\frac{\partial u_1}{\partial x_3} + \frac{\partial u_3}{\partial x_1})$ (middle column) and $\epsilon_{23} = \frac{1}{2}(\frac{\partial u_2}{\partial x_3} + \frac{\partial u_3}{\partial x_2})$ (right column) of the strain tensor ε.

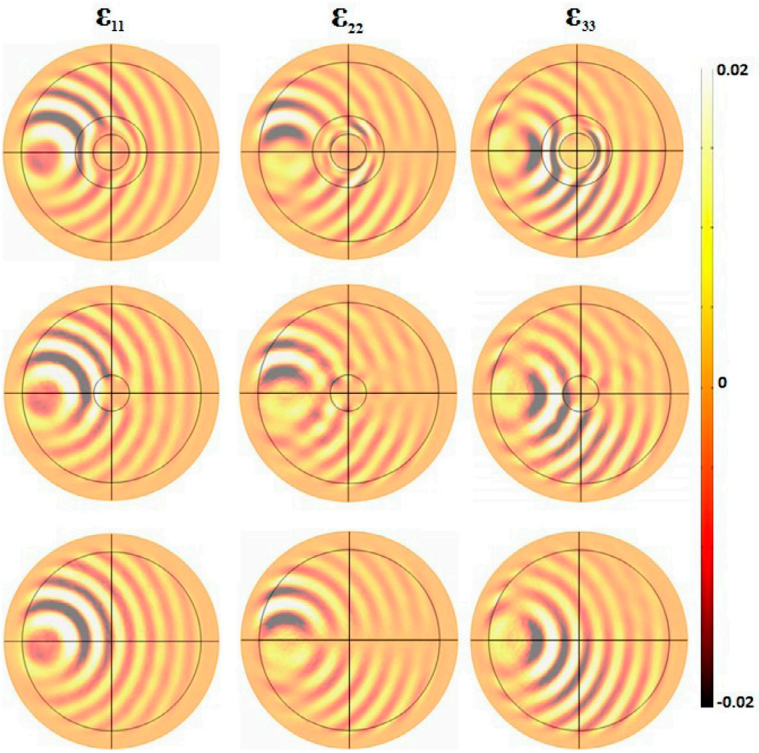

Figure 3. Deformation of an isotropic elastic medium (lower row), a soft spherical obstacle (middle row) and the same obstacle surrounded by an elastic cloak (upper row) for the same geometrical and elastic parameters and the same source (and frequency) as in figure 2. Real part of the deformation components $\varepsilon_{11} = \frac{\partial u_1}{\partial x_1}$ (left column), $\varepsilon_{22} = \frac{\partial u_2}{\partial x_2}$ (middle column) and $\varepsilon_{33} = \frac{\partial u_3}{\partial x_3}$ (right column) of the strain tensor ε.

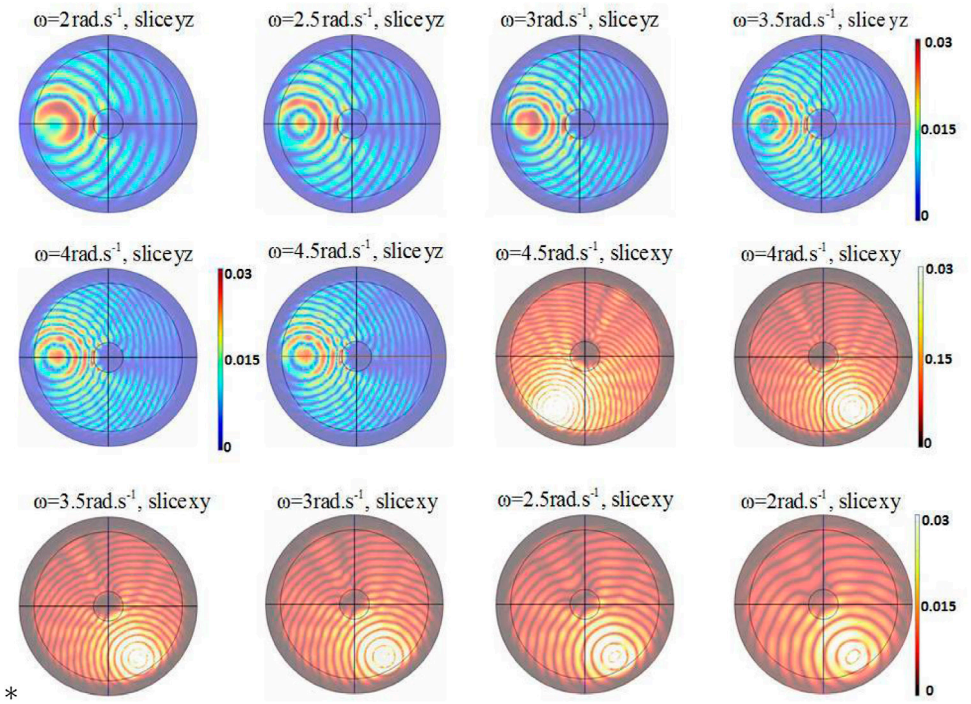

Figure 4. Real part of complex valued magnitude $\sqrt{u_1^2+u_2^2+u_3^2}$ of the elastic displacement for a time-harmonic point source oriented along the direction (1,1,1), in the frequency range $\omega = 2$–4.5 rad $\cdot$ s^{-1}, located at a distance $r = 8.062$ m from the center of a spherical soft sphere (without a surrounding cloak), with parameters as in figure 2.

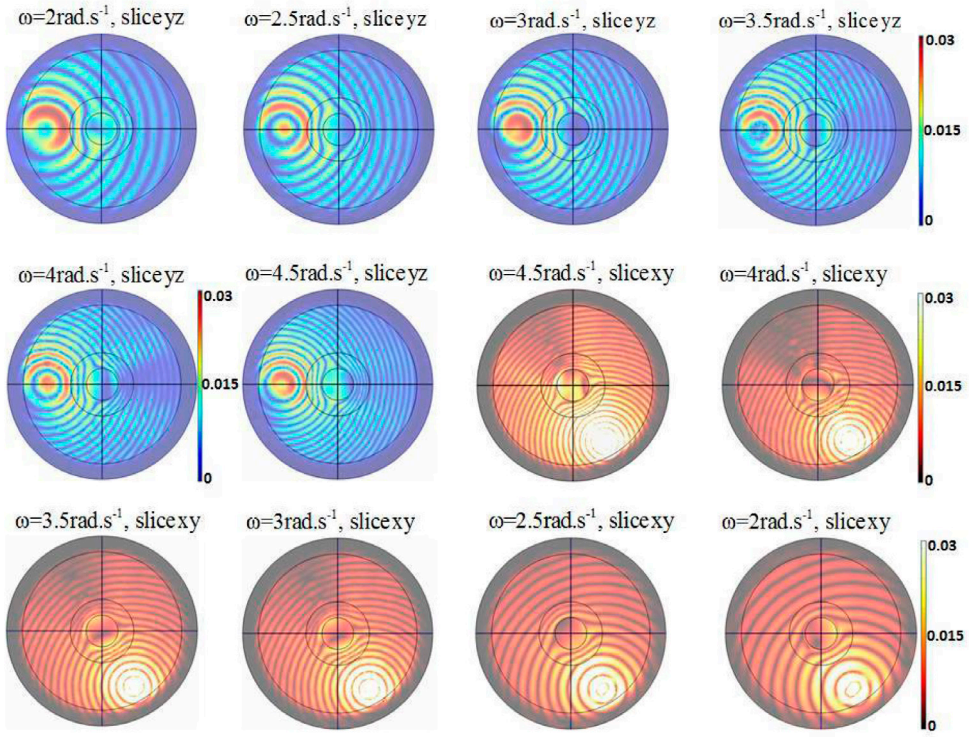

Figure 5. Real part of complex valued magnitude $\sqrt{u_1^2+u_2^2+u_3^2}$ of the elastic displacement for a time-harmonic point source in the frequency range $\omega = 2$–4.5 rad $\cdot$ s^{-1} located at a distance $r = 8.062$ m from the center of a spherical soft sphere and oriented along (1,1,1), with a surrounding cloak with parameters as in figure 2.

space), we plot in figure 7 the L^2-norm of the elastic displacement field within the sphere for given frequencies (see curves 1 to 7) against the parameter η. We conclude that the most favorable pair of parameters lies within an interval centered at $\omega = 3$ rad $\cdot$ s^{-1} and $\eta = 0.1$, which are indeed the values used in figures 2–6. A further quantitative investigation of

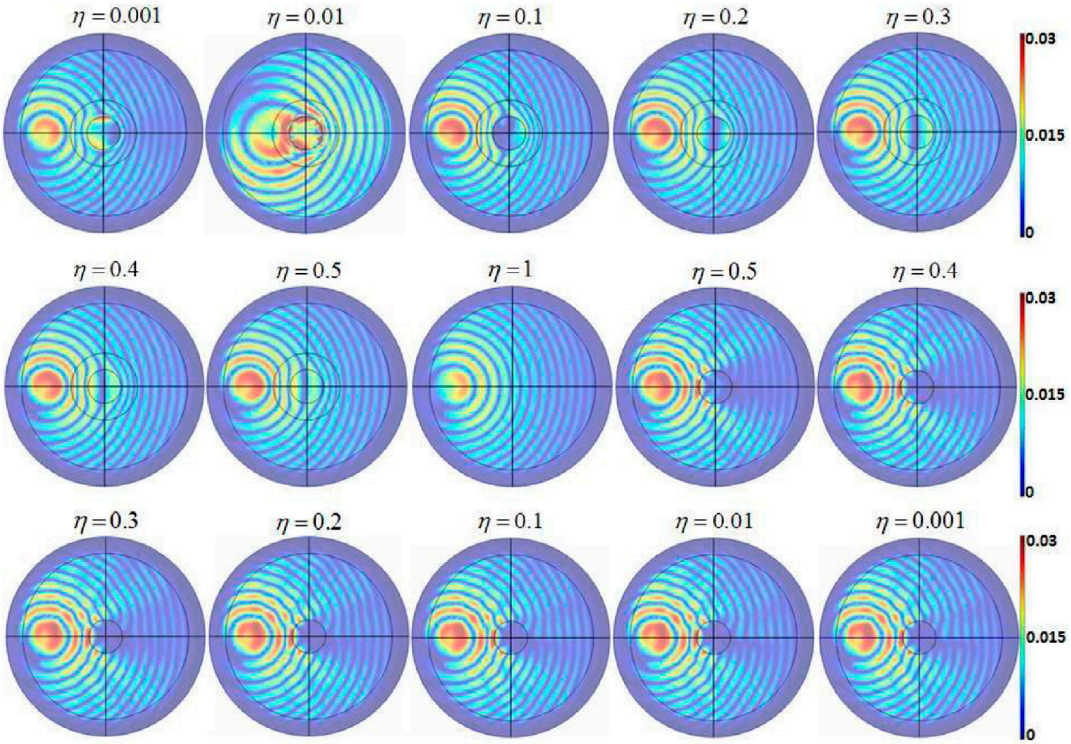

Figure 6. Spherical cloak (upper row and the first two images to the left of the middle row) with elastic parameters as in (8) and (7) of outer radius 4m dressing a soft sphere of radius 2 m with Lamé parameters $\mu = \eta, \lambda = 2.3\eta$ and $\rho = \eta^3$, with $\eta = 0.001,\ 0.01,\ 0.1,\ 0.2,\ 0.3,\ 0.4,\ 0.5$ and the same soft sphere alone (third row and the last two images of the middle row) within a homogeneous isotropic medium with Lamé parameters $\mu = 1, \lambda = 2.3$ and $\rho = 1$. Numerical illustration of the real part of a complex valued magnitude $\sqrt{u_1^2 + u_2^2 + u_3^2}$ of the elastic displacement, for a time-harmonic point source oriented along (1,1,1) at the frequency $\omega = 3\,\text{rad} \cdot \text{s}^{-1}$ located at a distance $r = 8.062$ m from the center of the soft sphere. Note that the isotropic homogeneous elastic material in the central panel ($\eta = 1$) serves as a benchmark.

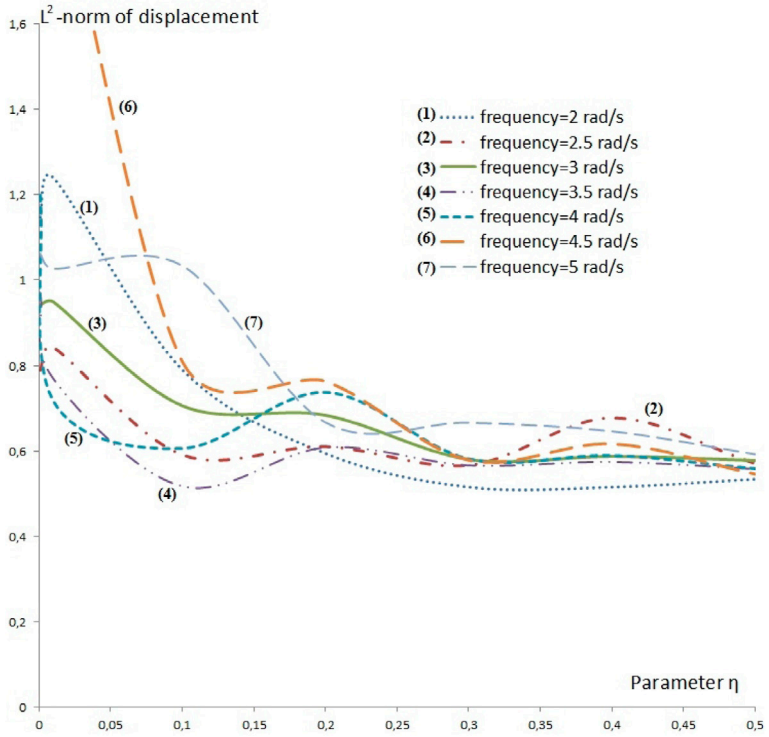

Figure 7. L^2-norm $\|\mathbf{u}\|_{L^2} = \sqrt{\int (u_1\bar{u}_1 + u_2\bar{u}_2 + u_3\bar{u}_3)}$ of the displacement field inside the small isotropic homogeneous soft balls of radius $r_1 = 2\ m$ surrounded by cloak of outer radius $r_2 = 4\ m$, against the parameter η varying from 0.001 to 0.5, for the same point force as in figure 6.

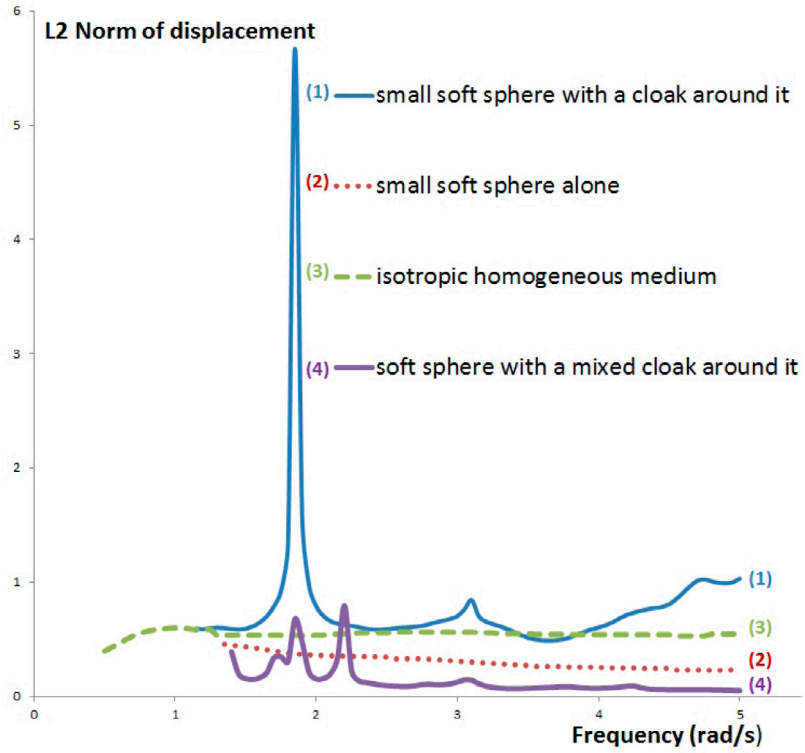

Figure 8. L^2-norm $\|\mathbf{u}\|_{L^2} = \sqrt{\int_{B(\mathbf{0},r_1)}(u_1\bar{u_1} + u_2\bar{u_2} + u_3\bar{u_3})}$ of the displacement field inside the small soft ball of radius $r_1 = 2$ *m*, for the fixed value $\eta = 0.1$, when (1) surrounded by the cloak of outer radius $r_2 = 4$ m, (2) alone, (3) when its elastic properties are replaced by those of the ambient isotropic homogeneous elastic medium, and (4) when it is now surrounded by a mixed cloak (made of 2 heterogeneous anisotropic layers: the same cloak as in (1) completed by a spherical region of inner radius $r_1 = 1.5$ m and outer radius $r_2 = 2$ m containing PML), the L^2 being computed over the sphere of radius 2 m (PML + soft obstacle). The frequency varies by 0.05 rad $\cdot$ s^{-1}. The point force is as in figure 6. The cloaked sphere being soft allows for a better highlight of the existence of resonance peaks in the case of an ordinary cloak (1). This clearly demonstrates the lack of wave protection within the cloaked soft sphere, for some resonances. However, when the same soft sphere is surrounded by a mixed cloak (4), the large resonance (1) is reduced by a factor greater than 6. Note also that a good wave protection is achieved for all other frequencies.

the favorable case $\eta = 0.1$, still exhibits some large peaks of values of the L^2-norm of the displacement field within the cloaked soft sphere, yet due to some resonances, as shown in figure 8. In the same vein, figures 5 and 6, show qualitative studies for the case $\eta = 0.1$ (ω varying) and $\omega = 3$ rad $\cdot$ s^{-1} (η varying), respectively. We can conclusively say that our cloak works well in terms of invisibility but does not offer a wave protection at all frequencies. We shall indeed see in the next section 5, that the cloak actually makes a concentrator for elastic fields at specific frequencies. In section 6 we shall propose a new generation of cloaks, termed here mixed cloaks, that offer a more accomplished wave protection.

5. Estimate of local resonance inside the cloak

We would like to gain some physical insight in trapped eigenstates within the core of the cloaks, which play an antagonistic role in seismic wave protection, as it transpires in figure 5. To do this, the governing equations associated with the invisibility cloak should be simplified, and a way to achieve this is by assuming that the Lamé parameter $\lambda = 0$ (vanishing compressibility modulus) and $\mathbf{u} = \mathbf{u}(r)$ (this seems legitimate in view of the fact that the problem is radially symmetric), then the three components of the displacement field are all solutions of the scalar Helmholtz equation in spherical coordinates:

$$\frac{\partial}{\partial r}\left(r^2\mu_r\frac{\partial}{\partial r}u_i\right) + \frac{\mu_\theta}{\sin\theta}\frac{\partial}{\partial\theta}\left(\sin\theta\frac{\partial}{\partial\theta}u_i\right) + \frac{\mu_\phi}{\sin^2\theta}\frac{\partial^2}{\partial^2\phi}u_i + \omega^2\rho u_i = 0 \tag{13}$$

where $\mu_r(r) = \mu_0(r - r_1)^2/r^2$, $\mu_\theta(r) = \mu_\phi(r) = \mu_0 r_2/(r_2 - r_1)$ and $\rho(r) = \rho_0((r - r_1)^2/r^2)(r_2^3/(r_2 - r_1)^3)$. The general solution of (13) is expressed in terms of spherical Bessel functions of first and second kinds:

$$u_i(r) = AJ_0\left(\frac{(r - r_1)\omega\rho_0 r_2^3}{\mu_0(r_2 - r_1)^3}\right) + BY_0\left(\frac{(r - r_1)\omega\rho_0 r_2^3}{\mu_0(r_2 - r_1)^3}\right). \tag{14}$$

It remains to supply the simplified governing equation (13) with two boundary conditions to find a particular solution (i.e. estimate the two constants A and B in (14)). At this stage, we use our physical intuition and make the hypothesis that some of the trapped eigenstates in figures 5 and 6 can be approximated by a simple spring-mass model: upon resonance, the shell of the cloak behaves like an effective spring, connected to a stress-free cavity (a mass) at the inner boundary r_1 and to

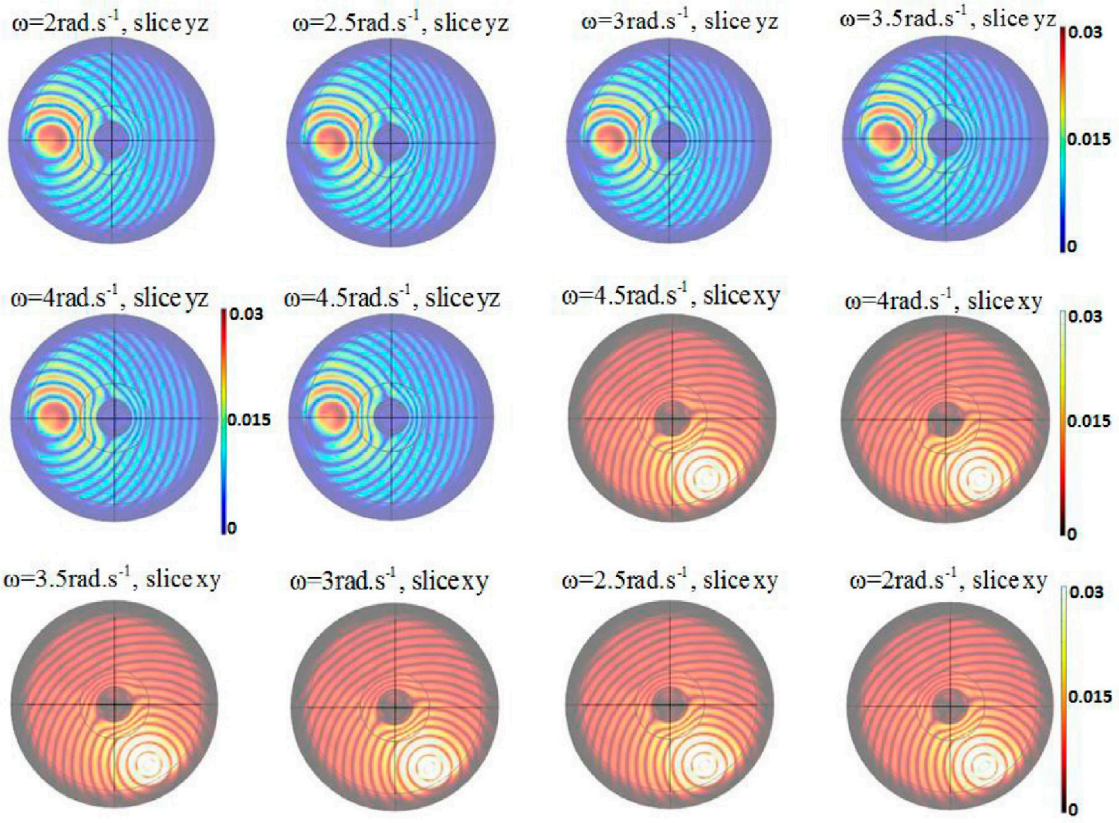

Figure 9. Mixed cloak: Real part of complex valued magnitude $\sqrt{u_1^2+u_2^2+u_3^2}$ of the elastic displacement for a time-harmonic point source in the frequency range $\omega = 2$–4.5 rad $\cdot$ s^{-1} located at a distance $r = 8.062$ m from the center of a soft sphere and oriented along (1,1,1), with a surrounding mixed cloak, consisting of an ordinary spherical Cosserat cloak of inner radius $r_1 = 2$ m and outer radius $r_2 = 4$ m and a PML region of inner radius $r_1 = 1.5$ m and outer radius $r_2 = 2$ m. The parameters are as in figure 2. One clearly realizes the absence of field inside the cloaked area, entailing a complete protection for the soft sphere. Compare figure 5.

a clamped wall at the outer boundary r_2. This effective model is inspired by almost trapped eigenstates unveiled in [24, 25] for Neumann-type cavities in the context of quantum cloaking (Schrödinger operator). Then, assuming that $\mathrm{d}u_i(r_1)/\mathrm{d}r = 0$ (stress-free boundary condition at the inner boundary of the cloak i.e. freely moving body inside the core) and $u_i(r_2) = 0$ (clamped boundary condition at the outer boundary of the cloak i.e. vanishing displacement field outside the cloak) for all three components, we find that the eigenfrequency should satisfy the following equation

$$Y_0(\omega r_2\sqrt{\mu_0/\rho_0})/J_0(\omega r_2\sqrt{\mu_0/\rho_0}) = 0, \qquad (15)$$

which gives the frequency estimate $\omega \sim 1.52$ rad $\cdot$ s^{-1} for $\mu_0 = \rho_0 = 1$ since the first zero of $Y_0(x)$ is 3.8317. This frequency estimate is in reasonable agreement with the finite elements' solution $\omega = 1.85$ rad $\cdot$ s^{-1} for the first resonance, which corresponds to the large elastic field enhancement shown in figure 8. The frequency estimate for the second resonance is $\omega \sim 2.79$ rad $\cdot$ s^{-1} since the second zero of $Y_0(x)$ is 7.0156 and this is also in reasonable agreement with the finite element's solution 3.1 rad $\cdot$ s^{-1}, which corresponds to the second peak in figure 8. The discrepancy between asymptotics and numerics could also be attributed to some unavoidable shift in resonances induced by the absorption within the PML (wherein the elastic parameters have a small imaginary part in order to damp the outgoing waves). Indeed, one should note that in figures 7 and 8 that we compute a real valued L^2-norm of the complex valued elastic displacement $\mathbf{u}$ by multiplying its components u_i by their complex conjugates $\bar{u}_i$. However, if we now choose to compute the complex valued quantity $\mathcal{N}(\mathbf{u}) = \int_\Omega \sqrt{u_1^2+u_2^2+u_3^2}$ and then take its real part $\Re(\mathcal{N}(\mathbf{u}))$, then it transpires from figures 7 and B2 that although the overall patterns of curves are preserved, there is a noticeable shift induced in the frequency corresponding to the global minimum of elastic displacement norm within the soft sphere for η ranging from 0.001 to 0.5. Indeed, this global minimum occurs at $\eta = 0.1$ for a frequency around $\omega = 3$ rad $\cdot$ s^{-1} in figure B2, instead of $\eta = 0.1$ for a frequency around $\omega = 3.5$ rad $\cdot$ s^{-1} in figure 7 for the real valued L^2-norm. We note again that these local resonances (that were not foreseen in [19] since we considered cloaked voids) are reminiscent of those unveiled in [24, 25] in the context of almost trapped eigenstates in quantum cloaking and sensors. This suggests some sensing potential in elastic waves.

6. The mixed cloak

In the previous sections, we have singled out the existence of an enhanced field inside the cloaked area, brought in by some

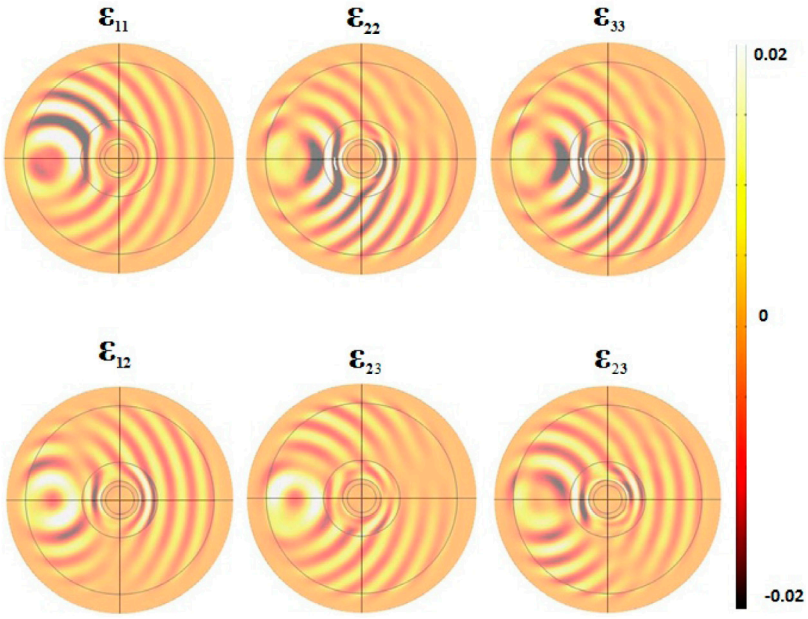

Figure 10. Deformation of a homogeneous isotropic elastic medium $\mu = 1$, $\lambda = 2.3$ and $\rho = 1$, containing a soft homogeneous isotropic spherical obstacle of radius 1.5 m with Lamé parameters $\mu = \eta$, $\lambda = 2.3\eta$ and $\rho = \eta^3$ for $\eta = 0.1$, surrounded by a mixed cloak with an elasticity tensor without the minor symmetries. The mixed cloak is made of an ordinary spherical Cosserat cloak of inner radius $r_1 = 2$ m and outer radius $r_2 = 4$ m, completed by a PML region of inner radius $r_1 = 1.5$ m and outer radius $r_2 = 2$ m. We apply a concentrated load of polarization (1,1,1) with frequency $\omega = 3$ rad $\cdot$ s^{-1} located in a homogeneous isotropic medium at a distance 8.062 m from the origin. Real part of the deformation components $\varepsilon_{ij} = \frac{1}{2}(\frac{\partial u_i}{\partial x_j} + \frac{\partial u_j}{\partial x_i})$, with $i,j = 1,2,3$, of the strain tensor ε. Compare with figures 2 and 3.

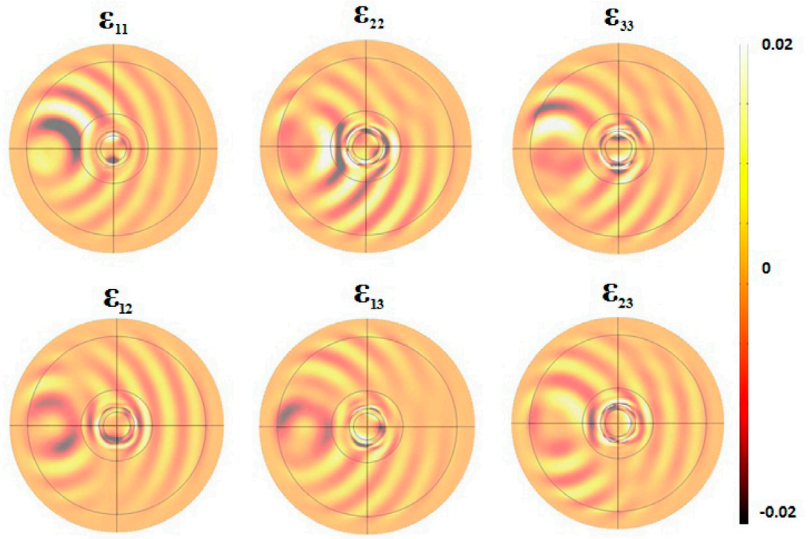

Figure 11. Deformation of a homogeneous isotropic elastic medium $\mu = 1$, $\lambda = 2.3$ and $\rho = 1$, containing a soft homogeneous isotropic spherical obstacle of radius 1.5 m with Lamé parameters $\mu = \eta$, $\lambda = 2.3\eta$ and $\rho = \eta^3$ for $\eta = 0.1$, surrounded by a mixed cloak with an elasticity tensor without the minor symmetries. The mixed cloak is made an ordinary spherical Cosserat cloak of inner radius $r_1 = 2$ m and outer radius $r_2 = 4$ m, completed a PML region of inner radius $r_1 = 1.5$ m and outer radius $r_2 = 2$ m. We apply a concentrated load (with frequency tuned to the peak $\omega = 2.20$ rad $\cdot$ s^{-1}, as seen on figure 8) of polarization (1,1,1) located in a homogeneous isotropic medium at a distance 8.062 m from the origin. Real part of the deformation components $\varepsilon_{ij} = \frac{1}{2}(\frac{\partial u_i}{\partial x_j} + \frac{\partial u_j}{\partial x_i})$, with $i,j = 1,2,3$, of the strain tensor ε. Compare with figures 2 and 3.

resonances. One of the purposes of the use of soft spheres in the present work is their ability to allow for a better highlight of the existence of resonance peaks and hence the possible lack of wave protection within the cloaked regions. Through an investigation of trapped modes in elasticity, some reasonably good asymptotic approximation of such (countable set of) resonances is supplied in section 5, as a solution of some transcendental equation. In this section, we propose a new generation

of cloaks, the mixed cloaks, in order to achieve cloaking along with protection for elastic (volume) waves. Such a protection might prove very useful in civil engineering. Indeed, such mixed cloaks overcome the pitfall of inner resonances (trapped modes) of elastodynamic cloaks that might coincide with eigenfrequencies of the buildings to be protected.

The mixed cloaks we introduce here consist of non-singular cloaks supplemented by an inner shell made of a perfectly matched layer. These cloaks have the property to achieve both invisibility and protection (enhanced fields due to Mie type resonances inside the soft sphere are drastically attenuated). Figure 1 gives a description of the geometric construction of the mixed cloak. The coefficients of the elasticity tensor and the density in the cloak and the PML parts of the mixed cloak, are the same as in (8) and (12), respectively. Figures 8(4)–11 depict the corresponding numerical illustrations. Compared to the case of non-mixed (ordinary) cloaks discussed in the previous sections, one realizes the absence of field inside the cloaked area, entailing a protection for the soft sphere. The results of a comparative quantitative study between the different cases are illustrated in figure 8, where the evidence of a protection is seen. However, it should be noted that some reminiscence of the resonances persists in figures 8 and 11, which might be attributed to trapped modes within the PML itself. As they achieve both cloaking and protection throughout a large range of frequencies, mixed cloaks are thus foreseen to play an important role in the advent of real manufactured mechanical cloaks. A homogenization algorithm could be applied for both the PML and the cloak in order to seek existing materials for their practical realization. Such a concept of mixed cloaks is also valid in the case of singular cloaks (in that case, one need simply add a PML layer at the singular boundary). It can be extended to other waves areas in physics and engineering.

7. Conclusion

Finally, we would like to stress that main features of the spherical elastic cloaks which we designed are their capability to make a soft sphere placed inside invisible to incoming elastic waves, not from a wave protection viewpoint, but from a substantial scattering reduction standpoint. Applications in anti-earthquake devices would require some further analysis, insofar as the elastic field can be dramatically enhanced within the cloak compared to a soft sphere on its own (note in passing that we considered a simplified model for soft spheres with real valued density and Lamé constants, although we appreciate that these might be complex valued [26]). However, if one has in mind to make a cloak for the range of frequencies of earthquakes from 2 to 5 rad $\cdot$ s^{-1}, our design might form the elementary brick of a more elaborate seismic cloak, which might be designed with a different geometric transform. Moreover, the material parameters of our cloaks are not frequency dependent, which is another pitfall since in practice one would fabricate some locally resonant structured materials in order to achieve the required density and elasticity tensor within the cloak, and we were limited below 2 rad $\cdot$ s^{-1} by the accuracy of the spherical PML (the larger the wave wavelength, the more absorption needed in PML) and above 5 rad $\cdot$ s^{-1} we are limited by the computational resources (numerical computation at 10 rad $\cdot$ s^{-1} required about 2 million tetrahedral elements for a converged result). A lot remains to be explored outside this range of angular frequencies. However, our study opens a route to research in seismic metamaterials, which is a very immature (but fascinating) field [27, 28]. We finally note that recent advances in fabrication and characterization of elastic metamaterials [29–31] could foster experiments in an approximate 3D elastic cloak. Of course, the metamaterial would only be able in practice to display a strong anisotropy on the cloak's inner boundary and it would only work throughout a finite range of frequencies. Its properties could be derived for instance from an effective medium approach in a similar way to what was proposed [16] and experimentally validated [18] for elastic waves in thin plates. Another route would be to use pre-stressed elastic media which would naturally have the required elasticity tensor for cloaking to be fully operational over a broad range of frequencies [32, 33].

As an alternative to elastodynamic cloaks with inner resonances, we further introduced the concept of mixed cloaks that have an additional PML layer attached to the inner boundary of the cloak. This PML considerably reduces the amplitude of the trapped eigenstates within the invisibility region, without deteriorating the cloaking effect. In this way we achieved good protection against volume elastic wave over a broad range of frequencies. This concept of mixed cloaks could be further translated into other wave areas for similar protection purpose.

Acknowledgments

The authors acknowledge European funding through ERC Starting Grant ANAMORPHISM. The authors also wish to thank Dr. Younes Achaoui for insightful comments on wave propagation in solid media.

Appendix A. Tensors of elasticity and deformation in spherical coordinates

Let us recall that any isotropic (possibly heterogeneous) elastic medium can be described by three (possibly spatially varying) scalar valued parameters λ, μ and ρ, which are respectively the Lamé parameters characterizing the compressibility and shear moduli, and the density, of the medium. The first two parameters are enough to generate the 21 non-zero components of the fully symmetric elastic constitutive tensor $\mathbb{C}$ written in a spherical basis (the reader can compare these expressions with those of the asymmetric elasticity tensor in equation (8)), for a possibly heterogeneous isotropic medium, which are

$$\begin{aligned}
&C_{rrrr} = C_{\theta\theta\theta\theta} = C_{\phi\phi\phi\phi} = (\lambda + 2\mu),\\
&C_{rr\theta\theta} = C_{\theta\theta rr} = C_{rr\phi\phi} = C_{\phi\phi rr} = C_{\theta\theta\phi\phi} = C_{\phi\phi\theta\theta} = \lambda,\\
&C_{r\theta r\theta} = C_{r\phi r\phi} = C_{\theta r\theta r} = C_{\theta\phi\theta\phi} = C_{\phi r\phi r} = C_{\phi\theta\phi\theta}\\
&\qquad = C_{r\theta\theta r} = C_{\theta rr\theta} = C_{r\phi\phi r} = C_{\phi rr\phi} = C_{\theta\phi\phi\theta}\\
&\qquad = C_{\phi\theta\theta\phi} = \mu.
\end{aligned}$$

The gradient, of the displacement field $\mathbf{u} = (u_r, u_\theta, u_\phi)$, has the following entries in spherical coordinates

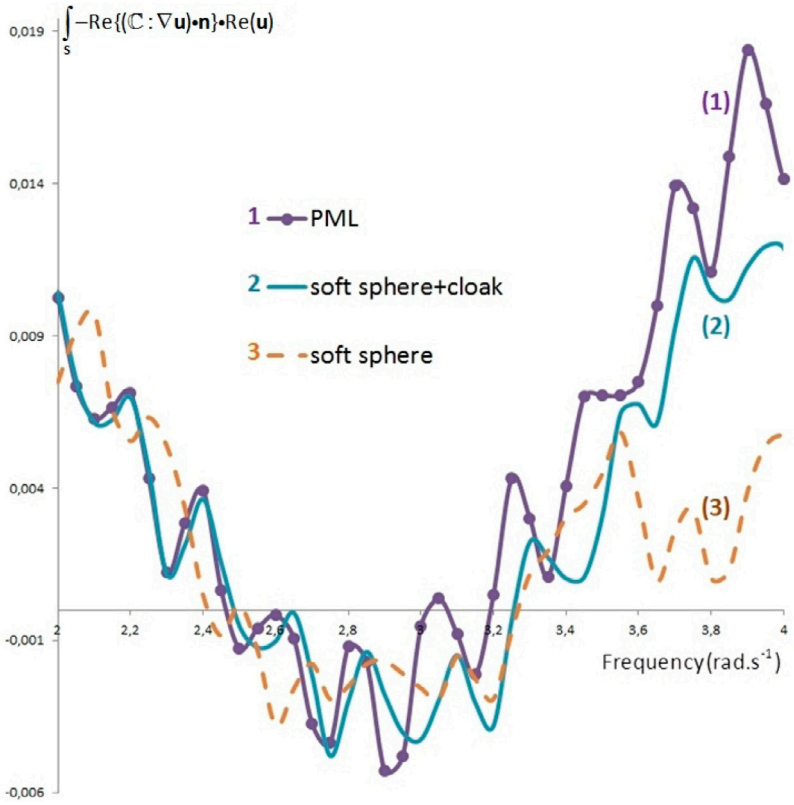

Figure B1. The integral $\int_S -\mathrm{Re}\,[(\mathbb{C} : \nabla \mathbf{u}) \cdot \mathbf{n}] \cdot \mathrm{Re}(\mathbf{u})$ over a surface of sphere S of radius 7 m, centered at the origin. A comparison between the isotropic homogeneous domain used as a benchmark (dotted curve (1)), the same domain now containing a soft sphere surrounded by a cloak (solid curve (2)) and a soft sphere alone (dashed curve (3)). Note that the frequency varies by a step of 0.05 rad $\cdot$ s^{-1}.

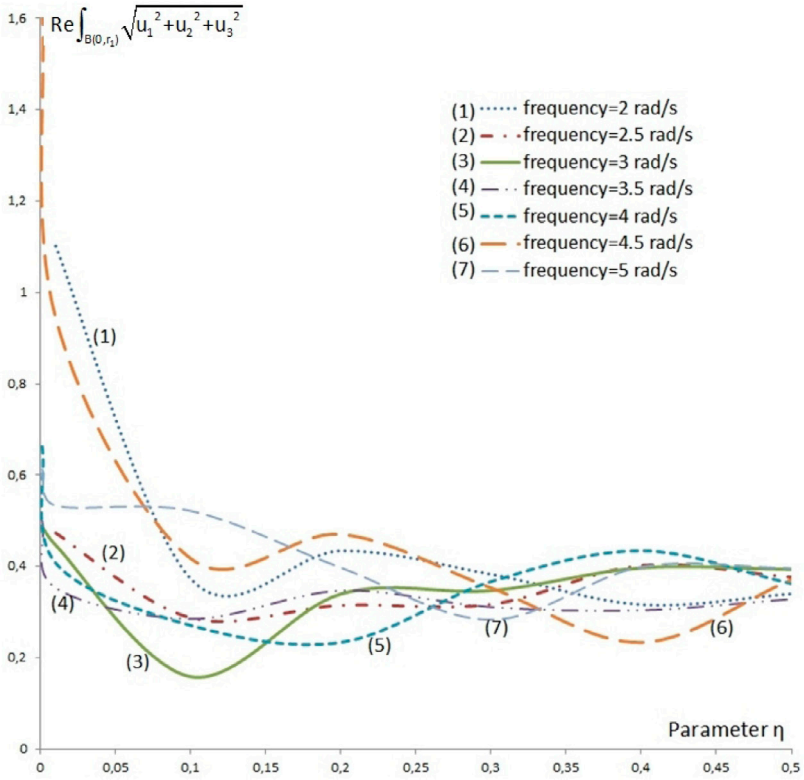

Figure B2. Real part of the complex valued quantity $\int_{B(\mathbf{0},r_1)} \sqrt{u_1^2 + u_2^2 + u_3^2}$ of the displacement field inside the small isotropic homogeneous soft balls of radius $r_1 = 2$ m surrounded by cloak of outer radius $r_2 = 4$ m, against the parameter η varying from 0.001 to 0.5, for the same point force as in figure 7. Note the shift in frequencies with figure 7 where the L^2-norm of displacement field was computed.

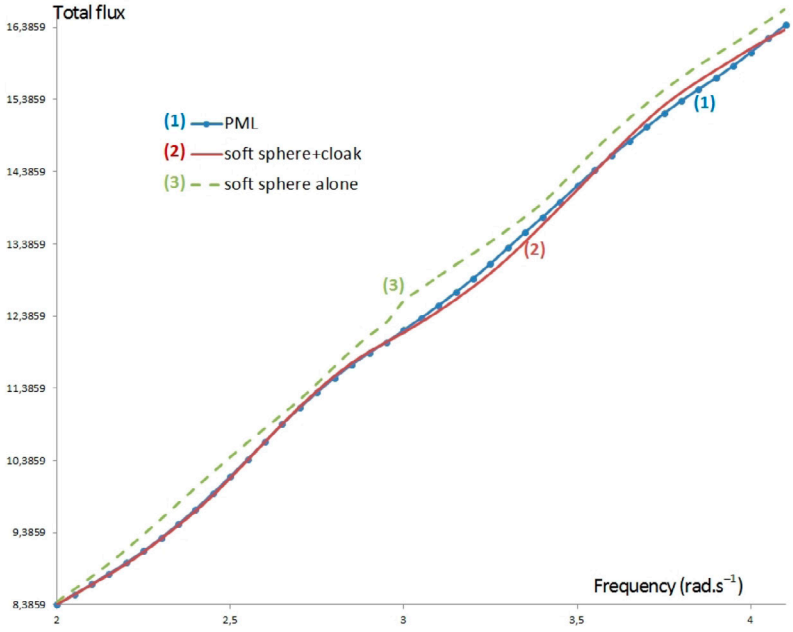

Figure B3. Total flux $\int_S |[(\mathbb{C} : \nabla \mathbf{u}) \cdot \mathbf{n}] \cdot \mathbf{n}|$ on the surface of a sphere S of radius 7 m, centered at the origin. A comparison between case (1) (solid line) of the isotropic homogeneous domain used as a benchmark, the same domain now containing a soft sphere with $\eta = 0.3$ surrounded by a cloak (dotted line (2)) and then a soft sphere alone (dashed line (3)). The point force is as in figure 6. The free elastic space (1) and cloaked soft sphere (2) curves are nearly superimposed, whereas the soft sphere alone (2) is clearly above them. Note that the frequency varies with a step of 0.05 rad $\cdot$ s^{-1}.

$$\nabla \mathbf{u} := \begin{pmatrix} \dfrac{\partial u_r}{\partial r} & \dfrac{\partial u_\theta}{\partial r} & \dfrac{\partial u_\phi}{\partial r} \\ \dfrac{1}{r}\dfrac{\partial u_r}{\partial \theta} - \dfrac{u_\theta}{r} & \dfrac{1}{r}\dfrac{\partial u_\theta}{\partial \theta} + \dfrac{u_r}{r} & \dfrac{1}{r}\dfrac{\partial u_\phi}{\partial \theta} \\ \dfrac{1}{r\sin\theta}\dfrac{\partial u_r}{\partial \phi} - \dfrac{u_\phi}{r} & \dfrac{1}{r\sin\theta}\dfrac{\partial u_\theta}{\partial \phi} - \dfrac{\cos\theta}{r\sin\theta}u_\phi & \dfrac{u_r}{r} + \dfrac{\cos\theta}{r\sin\theta}u_\theta + \dfrac{1}{r\sin\theta}\dfrac{\partial u_\phi}{\partial \phi} \end{pmatrix}. \tag{A.1}$$

Appendix B. Further numerics

We now complement numerical analysis discussed within the main text with additional quantitative—see figures B1–B3—evidence of cloaking. One notes that in figure B1 cloaking seems to degrade for frequencies higher than 2.8 rad $\cdot$ s^{-1}, which could be attributed to the fact that the mesh is no longer fine enough to ensure fully accurate numerical results (we have made some numerical tests to double-check this origin of inaccuracy).

Using a measure of flux of energy similar to that of Norris in equation (4.1) of [34] which is based upon the total field instead of the scattered field alone, we provide yet another numerical proof of suppression of scattering by the soft elastic sphere when it is surrounded by the cloak, see figure B1. We note that the dotted and solid curves, corresponding to elastic free space (1) and cloaked soft sphere (2) are nearly superimposed between 2 and 2.5 rad $\cdot$ s^{-1}, which tells us that numerics are fully accurate in this frequency range. However, for frequencies between 2.5 and 4 rad $\cdot$ s^{-1} curves (1) and (2) can be clearly told apart, an effect which could be attributed to the fact that the mesh is perhaps too loose to ensure full numerical convergence of the solution (we kept the same mesh for all frequencies). Nevertheless, the dashed curve (3) that corresponds to scattering by a soft sphere is always the curve farther apart from (1) Let us stress again that we have achieved this with spherical cloaks having elasticity tensors without the minor symmetries, akin to cosserat media [35].

References

[1] Pendry J B, Schurig D and Smith D R 2006 *Science* **312** 1780
[2] Leonhardt U 2006 *Science* **312** 1777
[3] Milton G W, Briane M and Willis J R 2006 *New J. Phys.* **8** 248
[4] Brun M, Guenneau S and Movchan A B 2009 *Appl. Phys. Lett.* **94** 061903
[5] Willis J R 1981 *Wave Motion* **3** 1–11
[6] Norris A N and Shuvalov A L 2011 *Wave Motion* **48** 525–38
[7] Craster R V and Guenneau S 2013 *Acoustic Metamaterials: Negative Refraction, Imaging, Lensing and Cloaking* (*Springer Series in Materials Science*) (New York: Springer)
[8] Farhat M, Enoch S, Guenneau S and Movchan A B 2008 *Phys. Rev. Lett.* **101** 134501
[9] Cummer S A and Schurig D 2007 *New J. Phys.* **9** 45
[10] Torrent D and Sanchez-Dehesa J 2007 *New J. Phys.* **9** 323
[11] Chen H and Chan C T 2007 *Appl. Phys. Lett.* **91** 183518
[12] Norris A 2008 *Proc. R. Soc.* A **464** 2411–34
[13] Cummer S A, Popa B-I, Schurig D, Smith D R, Pendry J, Rahm M and Starr A 2008 *Phys. Rev. Lett.* **100** 024301
[14] Christensen J and Garcia de Abajo F J 2012 *Phys. Rev. Lett.* **108** 124301
[15] Farhat M, Guenneau S and Enoch S 2009 *Phys. Rev. Lett.* **103** 024301
[16] Farhat M, Guenneau S and Enoch S 2012 *Phys. Rev.* B **85** 020301
[17] Guild M D, Alù A and Haberman M R 2011 *J. Acoust. Soc. Am.* **129** 1355–65

[18] Stenger N, Wilhelm M and Wegener M 2012 *Phys. Rev. Lett.* **108** 014301
[19] Diatta A and Guenneau S 2014 *Appl. Phys. Lett.* **105** 021901
[20] Jiang W X, Cui T J, Ma H F, Yang X M and Cheng Q 2011 *Appl. Phys. Lett.* **98** 204101
[21] Diatta A and Guenneau S 2015 Etude théorique et numérique du contrôle d'ondes élastiques dans des solides hétérogènes anisotropes *9th Colloquium of Association Francaise du Genie Parasismique (Paris, 30 November–2 December 2015)*
[22] Kohn R V, Shen H, Vogelius M S and Weinstein M I 2008 *Inverse Problems* **24** 015016
[23] Bigoni D, Serkov S K, Valentini M and Movchan A B 1998 *Int. J. Solids Struct.* **35** 3239–58
[24] Greenleaf A, Kurylev Y, Lassas M and Uhlmann G 2008 *Phys. Rev. Lett.* **101** 220404
[25] Greenleaf A, Kurylev Y, Lassas M and Uhlmann G 2011 *Phys. Rev.* E **83** 016603
[26] Palmeri M L, Sharma A C, Bouchard R R, Nightingale R W and Nightingale K R 2005 *IEEE Trans. Ultrason. Ferroelectr. Freq. Control* **52** 1699
[27] Kim S H and Das M P 2012 *Mod. Phys. Lett.* B **26** 1250105
[28] Brûlé S, Javelaud E H, Enoch S and Guenneau S 2014 *Phys. Rev. Lett.* **112** 133901
[29] Kadic M, Bückmann T, Stenger N, Thiel M and Wegener M 2012 *Appl. Phys. Lett.* **100** 191901
[30] Kadic M, Bückmann T, Schittny R and Wegener M 2013 *New J. Phys.* **15** 023029
[31] Bückmann T, Thiel M, Kadic M, Schittny R and Wegener M 2014 *Nat. Commun.* **5** 4130
[32] Norris A N and Parnell W J 2012 *Proc. R. Soc.* A **468** 2881–903
[33] Parnell W J 2012 *Proc. R. Soc.* A **468** 563–80
[34] Norris A N 1986 *Int. J. Eng. Sci.* **24** 1271–82
[35] Cosserat E and Cosserat F 1909 *Théorie des Corps déformables* (Paris: A. Hermann et fils)